IEEE P802.15
Wireless Personal Area Networks

Project	IEEE P802.15 Working Group for Wireless Personal Area Networks (WPANs)
Title	**UWB Channel measurements in Snow-Covered Environment**
Date Submitted	25 August 2004
Source	Julien Keignart and Norbert Daniele CEA-LETI DCIS/SMOC/LCARE 17 rue des Martyrs F 38054 Grenoble cedex 9 FRANCE Voice: (33)(0)4 38 78 58 88 Fax: (33)(0)4 38 78 51 59 E-mail: julien.keignart@cea.fr norbert.daniele@cea.fr
Re:	Response to call for Contributions on 15.4a Channel Modeling Subgroup
Abstract	In the frame of the IEEE 802.15-4a channel modeling subgroup up to 11 radio environments have been selected. This paper address the snow covered environment
Purpose	This document describe the measurement campaign done in a snow covered environment. Thanks to this campaign path loss exponent and a simple propagation model have been extracted.
Notice	
Release	

TABLE OF CONTENTS

I. INTRODUCTION

Thanks to the vicinity of our labs with high mountain area we have launched a UWB channel sounding measurement campaign in **TIGNES** (Savoie/France) ski resort. The measurements have been done close to the “Grande Motte” Glacier at an altitude of about 3000m. Mainly three kind of measurements have been done:

- Point to point measurements with antennas on the top of masts,
- Point to point measurements with antennas directly lied on the snow,
- Measurements with one antenna buried under snow.

This contribution concerns only the two first configurations.

II. METROLOGY : MEASUREMENT SETUP AND PROCEDURE

A. Time Domain Channel Sounder

On Transmitter side, a Pulse Pattern Generator (Anritsu MP1763C) with two additional filters allows us to fit the desired UWB impulse shape in the 3-5GHz bandwidth. The –3dB bandwidth corresponds exactly to 3.4GHz to 4.2GHz with a center frequency f_0=3.8GHz. Thanks to a power amplifier, the maximum radiated power corresponds to an impulse peak voltage equivalent to a sinusoidal wave of 30dBm (c.f. Figure 6 and Figure 7). This power can be tuned by varying the Pulse Pattern Generator output amplitude.

On Receiver side, we mainly use a wide band Digital Oscilloscope (LeCroy SDA6020) with a sampling rate of 20Gsps in real-time. In order to improve the time precision, a sinc interpolation is used in order to get a final time step of 5ps. Moreover, the signal is averaged over 16 snapshots for increasing the signal-to-noise ratio. For dynamic range consideration, it is also necessary to use a Low Noise Amplifier in front of oscilloscope input channel.

Both Transmitter and Receiver are connected to antennas with 3m cables. These antennas designed by LETI are compact omnidirectional ones, operational from 2.9GHz up to 12GHz. Antenna gain is equal to 0dB in horizontal plane, nevertheless more information concerning this gain will be described later.

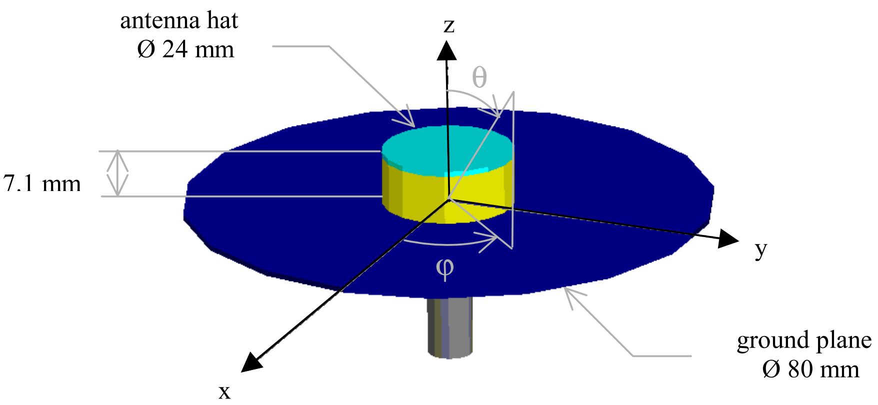

Figure 1 Compact Omnidirectional Antenna

The whole measurement link is illustrated in Figure 2. This time domain sounder allows to get a dynamic of 74dB with a Signal-To-Noise ratio higher than 25dB. This allows LOS link with antenna separation distance up to 30m (and up to 40m with a reduced Signal-To-Noise ratio). A view of the sounder is given in **Figure 3**, in the foreground one could see the pulse pattern generator, then the transmit antenna under the mast, finally, in the middle ground the receive antenna connected to the digital oscilloscope.

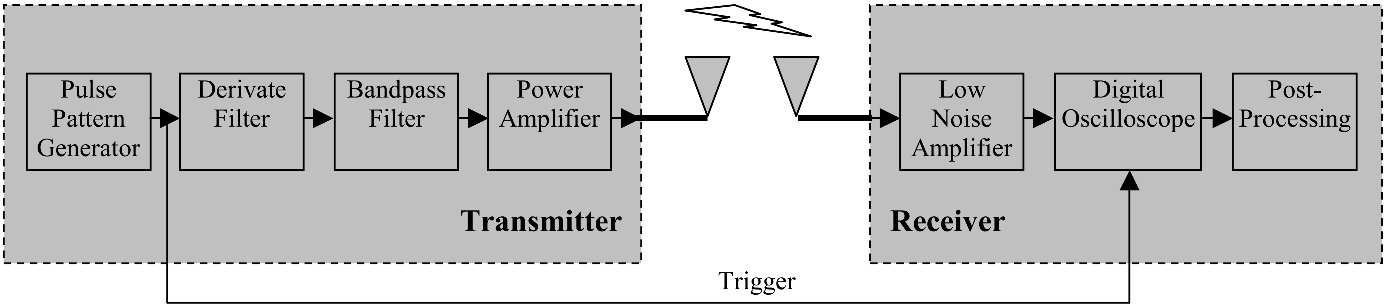

Figure 2 Channel sounder

Figure 3 Overall view of the sounder

As mentioned in introduction, two kind of measurements have been done: antenna on 1.3m high masts (44 measurements) and antenna at snow level (16 measurements). The measurement range d was comprised between 2m and 40m, for each experiment the receiver antenna was moved at two different places one meter around the main position. **Figure 4** illustrates the measurements configurations. The main measurements is in solid line, the complementary measurements are mentioned in black dotted line, the measurements at snow level are mentioned in blue doted line. **Figure 5** is a photography illustrating a measurement at snow level.

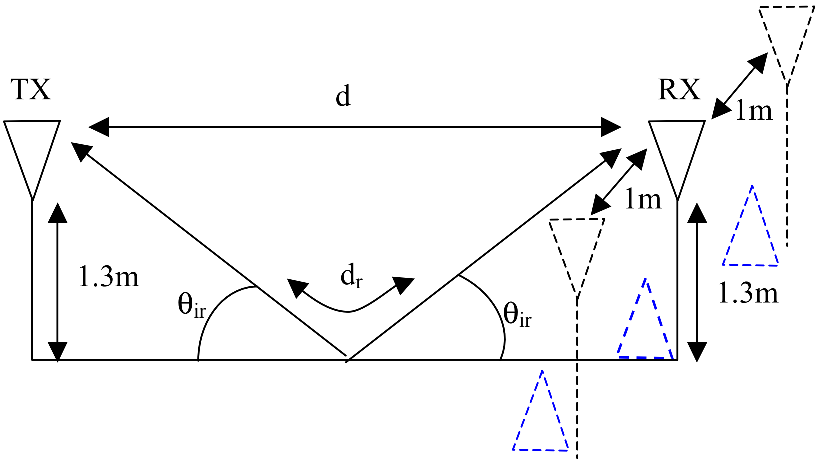

Figure 4 Measurements configurations

Figure 5 Snow level measurement example

B. Calibration

Contrary to Vector Network Analyzer measurements, with this kind of channel sounder the calibration procedure is not so obvious. The easiest way is to perform a reference measurement in anechoic chamber. The transmitter up to TX antenna is exactly the same for reference and all channel measurements; but, due to gain consideration, receiver link is different. From measurement performed in anechoic chamber, we deconvoluate (see III.A) all receiver elements before oscilloscope in order to get exclusively the "radiated" impulse including both antennas effects. This signal will be further called "Reference Signal". This "reference signal" is represented on **Figure 6** and **Figure 7** respectively in time and frequency domains.

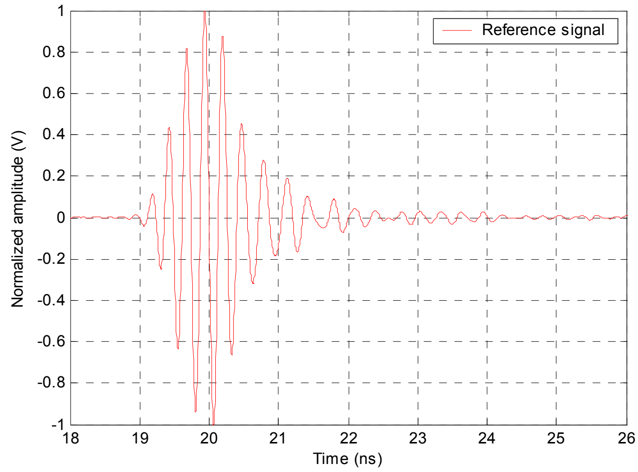

Figure 6 Reference signal in Time Domain

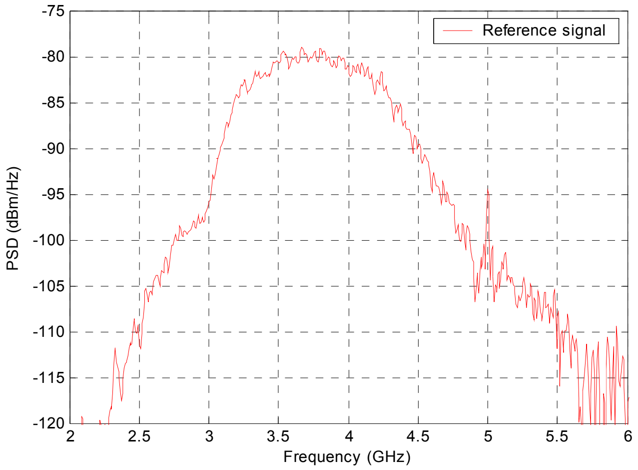

Figure 7 Power Spectrum Density of reference signal (in 10ns time window)

C. Environment

The environment was a quite flat area (about 2° slope) close to the funicular station for power supply needs. The snow thickness in the experimental area is varying from 0.5 m to 1.8m. It is to be noticed that the measurements have been done in July with a "summer snow". As the dielectric constant of snow is directly dependent of the wetness and dry snow density, this was the worst case in terms of loss under snow and reflection. Moreover during this period the snow layer is submitted to a daily transformation cycle due to the variation of the temperature during the day. The photography of the **Figure 8** shows the experimental environment, two cables are on the snow, one for the trigger and one for the AC power supply of the receiver.

Figure 8 Overview of the experimental environment

III. DATA ANALYSIS AND POST-PROCESSING

A. Main Post-processing

Like in calibration process, for all channel measurement it is firstly mandatory to deconvoluate effects of RX components (Cable and Low Noise Amplifier). The easiest way is to pass in frequency domain the measured signal. Effectively, each component can easily be measured in frequency with a Vector Network Analyzer (VNA). Then, a simple complex spectrum ratio is done. Then, the frequency signal is passed back to time domain thanks to passband Inverse Fourier Transform (Hermitian reconstruction). A complete description of this IFT method is available in [1] .

B. First Sight Comments

After a first brief analyze of the whole data sets, the channel impulse response is very poor in multi-path due to the environment properties. Only the direct line-of-sight path and the reflected path are “visible”. Consequently, exclusively path loss information in part III.C and more details concerning the reflected path III.D will be presented.
Several channel impulse responses are given in part III.E for antenna on 1.3m high masts and antenna separation of 2, 5, 10, 20, 25, 30 and 40 meters.

C. Path Loss Model

The path loss in dB as a function of distance (supposed frequency independent with $f = f_0$) is given by [2] :

$$PL_{dB}(d) = PL_{0dB} + 10n\log_{10}\left(\frac{d}{d_0}\right) + S$$
$$\text{with } d \geq d_0$$

In this equation d_0 is a reference distance equal to 1m, and the corresponding path loss is the interception point noted PL_0. The coefficient n is the path loss exponent equal to 2 in free-space environment. Finally, S is the shadowing fading parameter; it is a centered Gaussian distribution from which it is possible to extract its standard deviation σ_S.

In a first step, we have collected all the data corresponding to both antennas at 1.3m high. The path loss linear regression of these data is plotted on Figure 9. The fit is quite in good accordance with all data excepted highest values for which the Signal-To-Noise ratio is not so good.

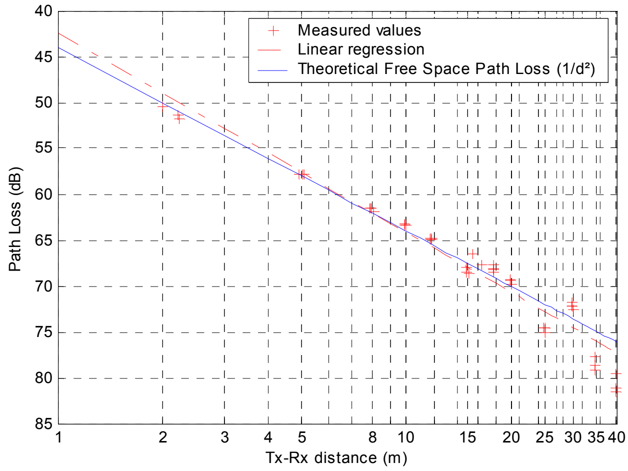

Figure 9 Path Loss as a function of distance (full range up to 40m)

In order to eliminate dispersion effects due to distances higher than 30m, we have plotted the path loss linear fit with a limited distance range on Figure 10.

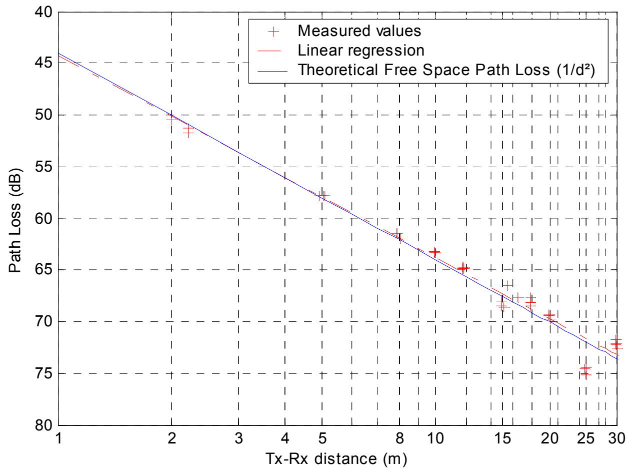

Figure 10 Path Loss as a function of distance (limited range up to 30m)

By calculating the shadowing standard deviation, we conclude that the second linear regression is much greater with a value of only 1.08dB. A path loss parameters values are available in Table 1.

Finally, the few measurements at snow level have been processed for getting path loss information (c.f. **Figure 11**). In this configuration, interpretation is not easy due to vicinity of snow, and no more details will be described in this paper.

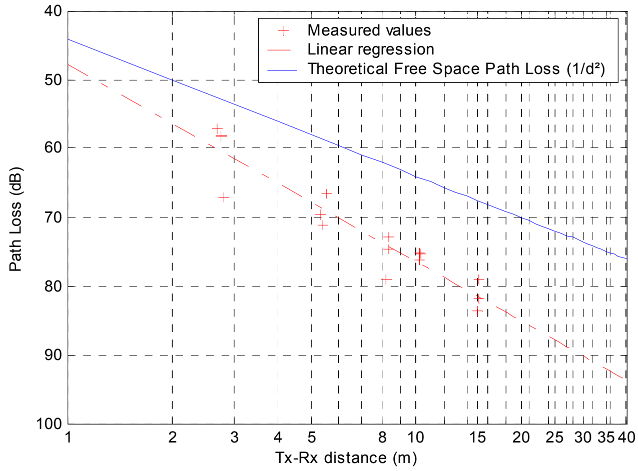

Figure 11 Path Loss as a function of distance with RX antenna at snow level

Configuration	Parameters		
	n	PL_0 (dB)	σ_S (dB)
Full range up to 40m	2.17	42.42	1.74
Limited range up to 30m	1.96	44.25	1.08
RX antenna at snow level	2.86	47.86	2.68

Table 1 Path Loss parameters

D. *Two-ray channel interpretation*

Due to investigated environment by considering in a first approximation the slope of the ground null, the classical definition of two-ray propagation can be useful to well understand the effect of second path. A full description of this model can be found in [3] . The direct ray and the ray reflected by the ground are considered, as illustrated in Figure 4.
The ground is regarded here as a plane surface, and the snow effect is included in its complex permittivity ε_r [4] taken in accordance to "summer snow" at frequency *f0*:

$$\varepsilon_r = \varepsilon_r^{'} - j\varepsilon_r^{''} \qquad \text{with} \qquad \varepsilon_r^{'} = 3 \text{ and } \varepsilon_r^{''} = 0.6$$

Then, due to the vertical polarization of our antennas, the reflection coefficient can be simplified to:

$$R_V = \frac{\varepsilon_r \sin\theta_{ir} - \sqrt{\varepsilon_r - \cos^2\theta_{ir}}}{\varepsilon_r \sin\theta_{ir} + \sqrt{\varepsilon_r - \cos^2\theta_{ir}}}$$

with θ_{ir} : incident and reflected angles supposed equal, see figure 4

By considering that the field at the receiver is the superposition of the contributions associated to the two rays, the path loss can be expressed as:

$$PL(d,f) = \left(\frac{4\pi f}{C}\right)^2 \left|\frac{e^{-jkd}}{d} + \frac{R_v e^{-jkd_r}}{d_r}\right|^{-2}$$ with d_r the distance of the reflected path

As previously, we suppose the path loss independent with the frequency by taking *f=f0*. Figure 12 represents the path loss effect for the direct-path and the reflected-path. The exact difference between these two curves is given for some distances in Table 2 as "Path Loss: Direct Versus Reflected Path".

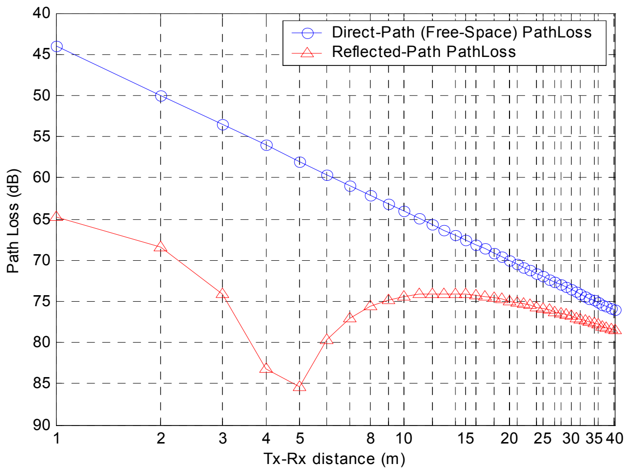

Figure 12 Two-ray model Path Loss

The theoretical time shift between the propagation delay corresponding to: direct path (distance d) and reflected path (distance d_r) is easily calculated by geometry with **Figure 4** dimensions. For each distance, this shift is reported in **Table 2** as "2nd path delay".

An other important effect to take into account is the antenna gain. Effectively, in the horizontal plane for the direct path the gain is 0dB, but concerning the reflected path it is wrong. The elevation angle need to be determinate for the different distances d. Then, the corresponding, antenna gain at the center frequency f_0 is obtain thanks to gain pattern measurements/simulations (c.f. **Figure 13**). All these values are reported in **Table 2**.

And finally in **Table 2**, the total losses due to path loss (with the simplified two-ray channel model) and antenna gain are calculated for the reflected path relatively to the direct path (noted "Losses: Direct Versus Reflected Path"). These values show that for short distances, the losses impacting the reflected path are very important and even more than our Signal-To-Noise ratio.

Effectively, on **Figure 14** for distances of 2 or 5 meters the reflected path is invisible whereas time shifts are higher than impulse duration. For distances of 10 meters and so on, the second path is visible by deforming the impulse due to a short time shift of 1ns or less, which represent delay smaller than the complete impulse duration. And the more, the distance increases, the more the second path amplitude increases compare to first path normalized amplitude.

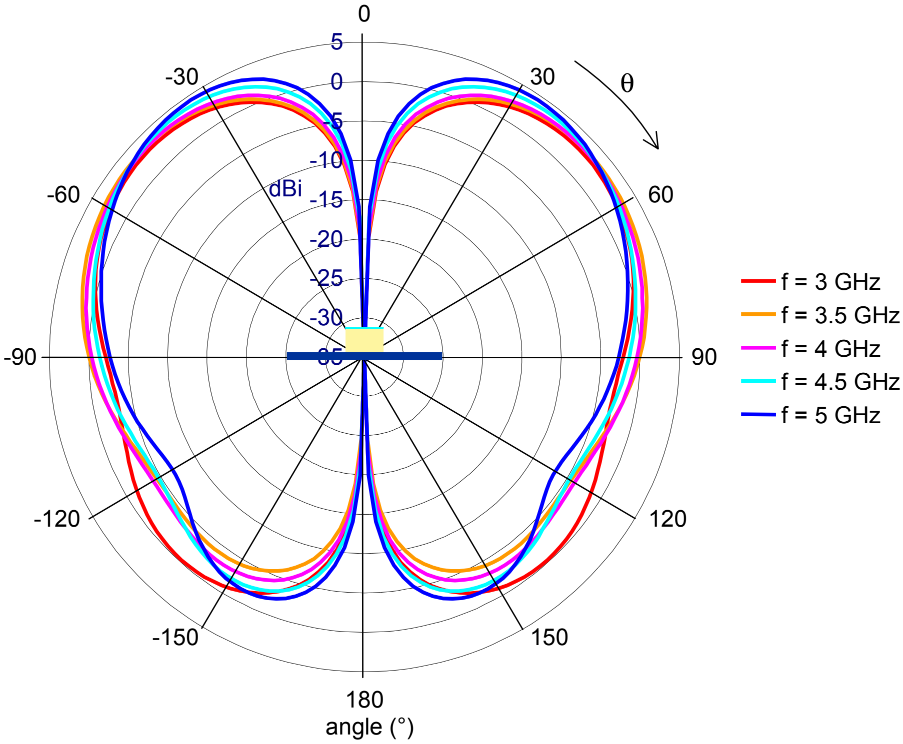

Figure 13 Gain pattern in elevation (x0z)

Tx-Rx distance (m)	**2**	**5**	**10**	**15**	**20**	**25**	**30**	**35**	**40**
2nd Path Elevation (θ°)	142.4	117.5	104.6	99.8	97.4	95.9	94.9	94.2	93.7
Antenna Gain (dB)	-3.32	-3.51	-2.00	-1.46	-1.2	-0.09	-0.08	-0.07	-0.06
2nd Path Delay (ns)	4.26	2.12	1.11	0.74	0.56	0.45	0.37	0.32	0.28
PathLoss: Direct VS Reflected Path (dB)	-18.40	-27.44	-10.39	-6.65	-4.91	-3.90	-3.23	-2.76	-2.41
Losses: Direct VS Reflected Path (dB) *	-25.04	-34.46	-14.39	-9.57	-7.31	-4.08	-3.39	-2.9	-2.53

* : include path loss difference and losses due to both antenna gain

Table 2 Direct path VS Reflected path as a function of distance

E. Channel impulse response examples

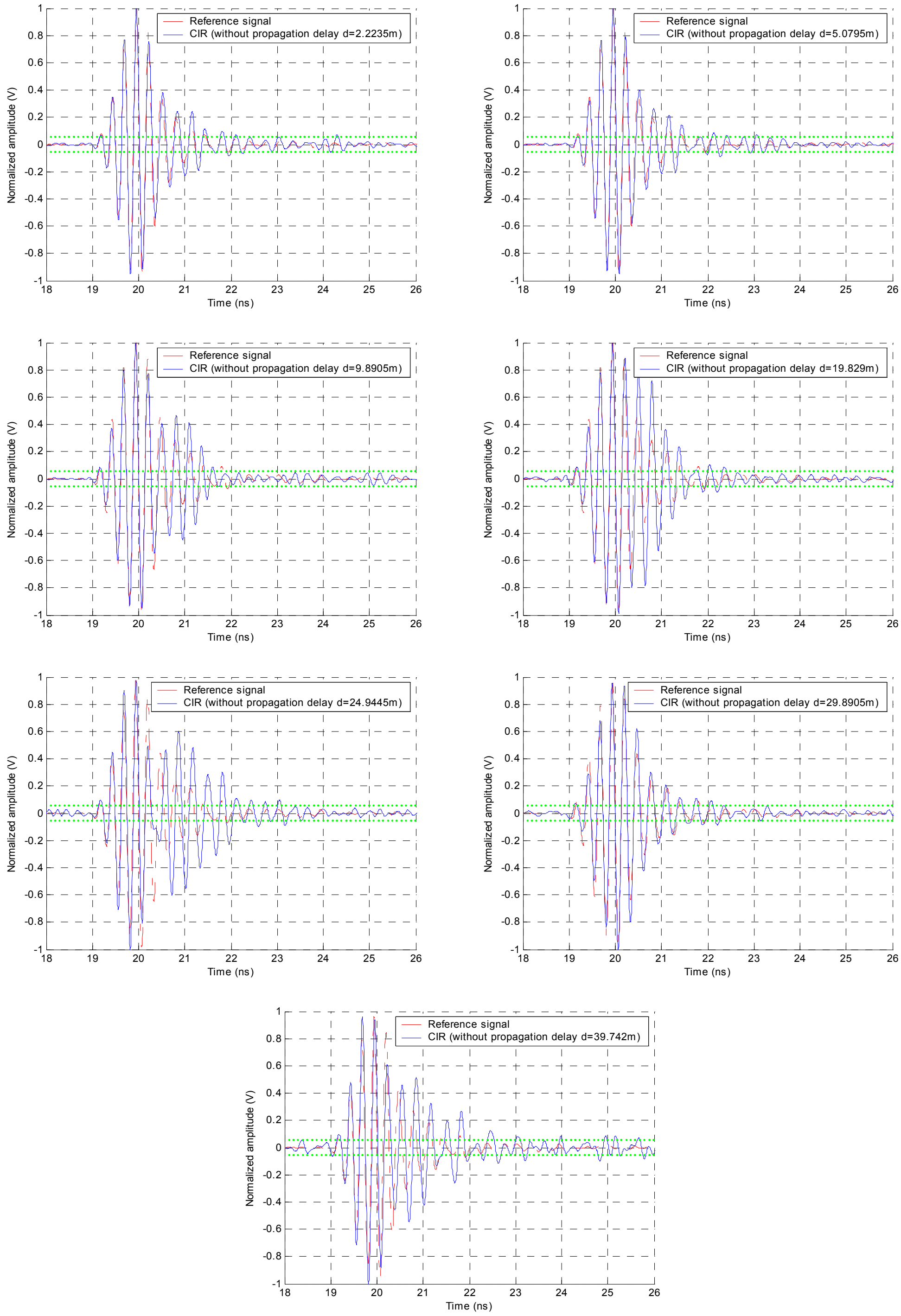

Figure 14 Channel impulse responses examples for some distances

IV. CONCLUSION

A time domain UWB channel sounding campaign in snow-covered environment has been done. This campaign allowed us to give interesting information about the snow influence on UWB channel impulse responses.

Essentially, path loss parameters have been extracted from these data: path loss exponent, interception point and shadowing fading standard deviation. Moreover, a simplified two-ray channel model has been used to well understand propagation phenomena. Finally, it is important to keep in mind that in the model proposed the amplitude of the reflected path is tightly linked to the characteristics of the snow layer, that is to say mainly wetness and dry snow density.

V. ACKNOWLEDGMENTS

Many thanks to the ski first-aid worker team of TIGNES for providing us with a nice snow area and a very good base camp at their first aid station.
We wish to thank also the TIGNES cable railway development company for their help in the transport of our heavy equipments.

VI. REFERENCES

[1] B. Denis and J. Keignart, ***"Post-processing framework for enhanced UWB channel modelling from band-limited measurements"***, in Proc. IEEE Conference UWB Systems and Technologies (UWBST03), Reston, VA, USA, Nov 2003, pp.260-264

[2] Chia-Chin Chong, Youngeil Kim and SeongSoo Lee, ***"UWB Channel Model for High Rise Apartments"***, IEEE P802.15-04-0306-00-004a, July 2004

[3] T.S. Rappaport, ***"Wireless Communications: Principles and Practice"***, Prentice Hall PTR, Second Edition 2002, pp.114-125

[4] F. Lemaitre and H.J. Mametsa, ***"Propagation à travers la neige"***, ONERA Centre d'Etudes et de Recherches de Toulouse, December 1991